**New Phytologist Supporting Information, The Arabidopsis mTERF-repeat MDA1 protein plays a dual function in transcription and stabilization of specific chloroplast transcripts within the *psbE* and *ndhH* operons,** Louis-Valentin Méteignier, Rabea Ghandour, Karin Meierhoff, Aude Zimmerman, Johana Chicher, Nicolas Baumberger, Abdelmalek Alioua, Jörg Meurer, Reimo Zoschke, Kamel Hammani. Accepted 15 April 2020

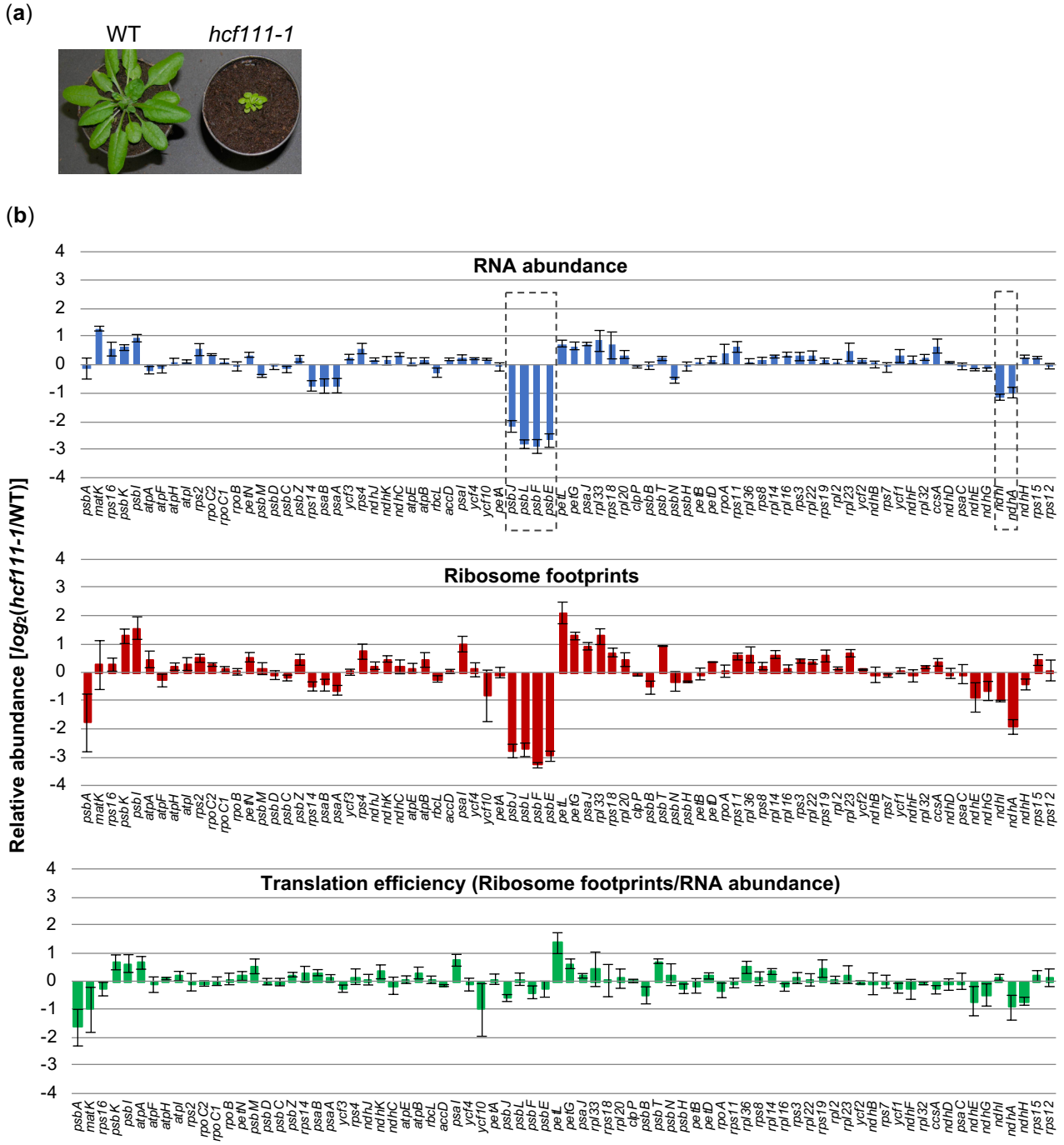


**Fig. S1 Phenotype and ribosome profiling analyses of the *mda1* mutant allele *hcf111-1*.** (a) Phenotype of 5 week-old *hcf111-1* and wild-type (WT) plants grown on soil. (b) Genome-wide analyses of chloroplast transcriptome and translation activity in *hcf111-1* was performed as previously described (Trosch *et al.*, 2018) for three biological replicates (vertical lines indicate standard deviation). The Ratio of relative RNA abundance (reflecting transcript levels), ribosome footprint levels (indicating translation output) and translation efficiencies (ribosome footprints normalized to transcript levels) of *hcf111-1* relative to the WT is plotted for all plastid-encoded reading frames.

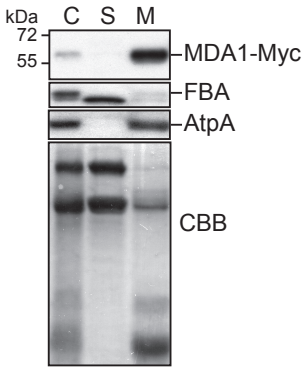


**Fig. S2. MDA1 is associated to membranes in chloroplasts.** Isolated chloroplasts were lysed in hypotonic buffer and membrane and soluble protein fractions were separated by centrifugation. 10 μg of chloroplast (C), soluble (S) and membrane (M) protein fractions were analyzed by immunoblotting using antibodies against Myc epitope, a stromal protein (Fructose-bisphosphate aldolase 1) and a membrane associated subunit of the ATP synthase complex (AtpA). The Coomassie Blue (CBB) stained membrane is shown below.

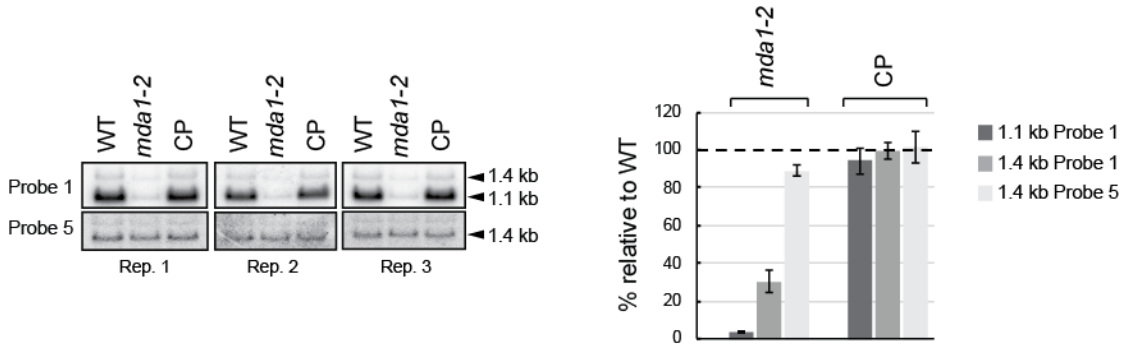


**Fig. S3. Quantification of the abundance of the 1.4 and 1.1 kb *psbE-F-L-J* mRNAs in the different plant genotypes by RNA blot analyses**. RNA blots were hybridized with probes specific to the *psbE* ORF (probe 1) or the 5' extension of the 1.4 kb mRNA (probe 5) as in Fig. 4. The percent changes relative to WT of the mRNA steady state levels are provided to the right. The accumulation of the 1.1 kb *psbE-F-L-J* mRNA is more severely affected than the 1.4 kb in the *mda1* mutant. Data are means of three independent experiments and standard errors are indicated.

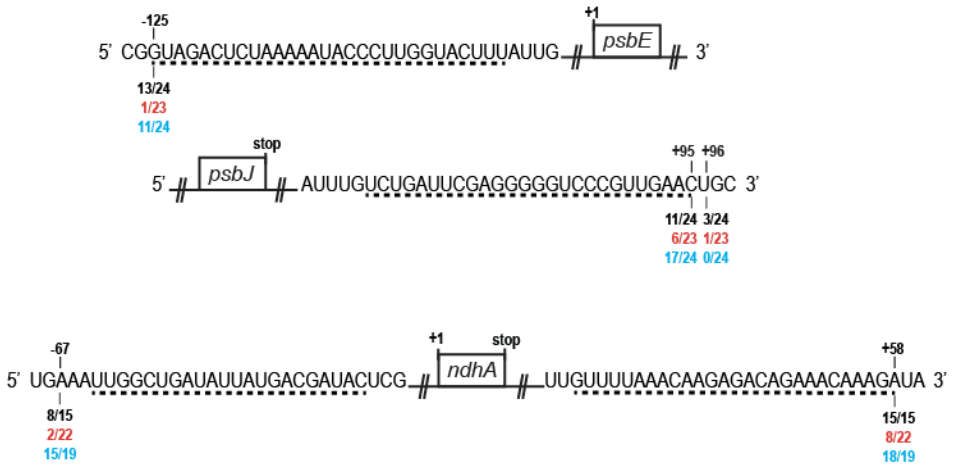


**Fig. S4. Genome mapping of the predominant *in vivo* 5'- and 3'-ends for the processed *psbE-J-L-J* and *ndhA* mRNAs determined by cRT-PCR in different genotypes.** The numbers of clones with the specified ends for the wild-type, *mda1* and complemented plants, are respectively indicated in black, red and blue. The positions are given according to the gene start codon (+1) for the 5' ends to the stop codon for the 3' ends. The sequences of the *in vivo* sRNAs that correspond to PPR footprints (Zhelyazkova *et al.*, 2012; Ruwe *et al.*, 2016) are dotted underlined.

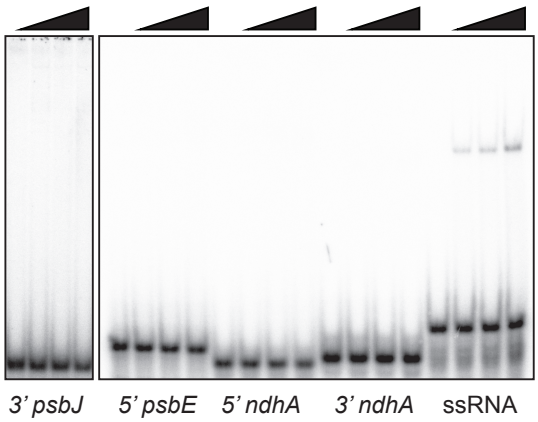


**Fig. S5. RNA gel mobility shift assays showing no binding of MDA1 to sRNAs.** Increasing amounts of rMDA1 (0, 100, 200 and 400 nM) were incubated with RNA sequences corresponding to sRNA footprints matching *psbE*, *ndhA* 5'- or *psbJ* and *ndhA* 3'-ends that accumulate in Arabidopsis chloroplasts. The 43-nt ssRNA probe used in Fig. 8c was used as a positive binding control. These ~20 nucleotides sRNAs are not predicted to adopt stable secondary structures and prevent MDA1 binding.

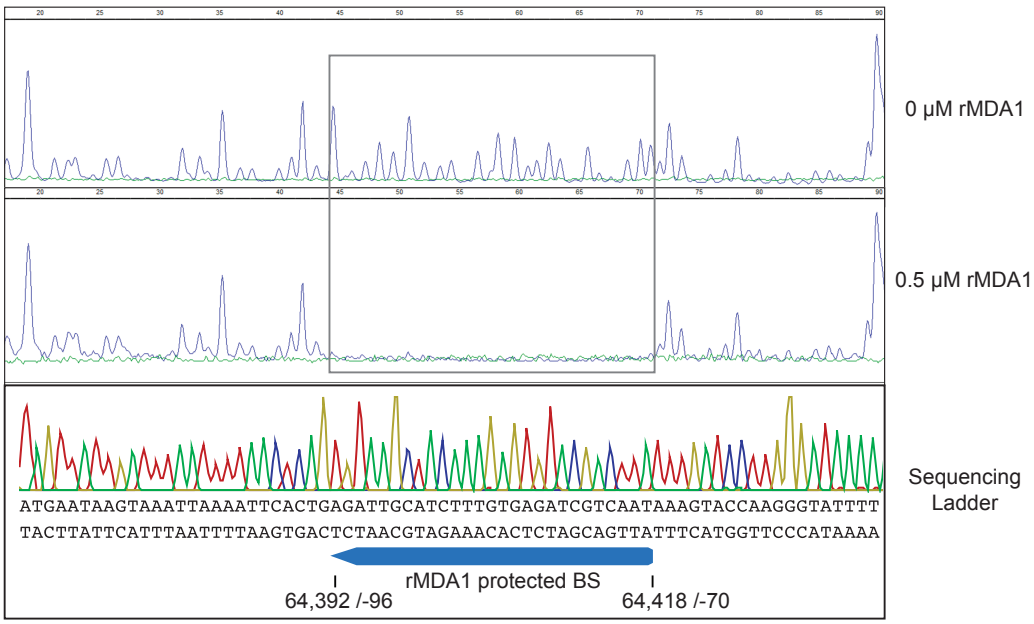


**Fig. S6. *psbE* DNAse footprinting assay.** A 6FAM-labelled PCR amplified *psbE* DNA fragment (E3 from Fig. 10) was partially digested with DNase I in presence or absence of rMDA1. Cleaved DNA fragments were fractionated by automated fluorescent capillary electrophoresis and product peaks were aligned to a sequencing ladder with GeneMapper software to map the DNAse protected binding site (BS) of rMDA1 (outlined with a box). The chloroplast genomic position of the BS is given according to the nucleotide sequence of the complete Arabidopsis genome NC_000932 or *psbE* start codon.

| | **WT** ($n_h$=5) | ***mda1-2*** (n=5) | ***hcf111*** (n=5) | ***mda1-2 CP*** (n=5) |
|---|---|---|---|---|
| **Fv/Fm**[a] | 0,81 ± 0,00 | 0,44 ± 0,00 | 0,46 ± 0,01 | 0,80 ± 0,00 |
| **Fo** | 1,00 ± 0,11 | 2,96 ± 0,32 | 3,02 ± 0,29 | 0,98 ± 0,08 |
| **$\Phi_{PSIIb}$** | 0,72 ± 0,01 | 0,28 ± 0,00 | 0,30 ± 0,03 | 0,70 ± 0,01 |
| **$NPQ_c$** | 0,19 ± 0,02 | 0,37 ± 0,04 | 0,31 ± 0,03 | 0,20 ± 0,03 |
| **$\Phi_{PSId}$** | 0,45 ± 0,02 | 0,34 ± 0,06 | 0,39 ± 0.08 | 0,44 ± 0,02 |
| **$\Phi_{PSI\ NDe}$** | 0,27 ± 0,05 | 0,64 ± 0,08 | 0,54 ± 0,03 | 0,26 ± 0,06 |
| **$\Phi_{PSI\ NAf}$** | 0,28 ± 0,03 | 0,02 ± 0,01 | 0,10 ± 0,05 | 0,30 ± 0,02 |
| **%[g] $\Delta A_{P700}$** | 100,00 ± 11,22 | 49,25 ± 7,90 | 38,45 ± 11,23 | 103,25 ± 14,05 |

[a]maximum quantum yield of PSII
[b]effective quantum yield of PSII (50 µmol photons $m^{-2}$ $s^{-1}$).
[c]non-photochemical quenching.
[d]quantum yield of PSI.
[e]quantum yield of non-photochemical energy dissipation due to donor side limitation.
[f]quantum yield of non-photochemical energy dissipation due to acceptor side limitation.
[G]maximum absorbance of P700 in % of the WT.
[h]number of plants measured.

**Table S2. Chlorophyll *a* fluorescence induction and light-induced PSI absorbance changes**. Chlorophyll *a* fluorescence was measured on 2-week-old Arabidopsis plants grown on soil. Representative measurements of chlorophyll *a* fluorescence in the WT, *mda1* mutants and complemented lines. Saturating light pulses were given in 20 s intervals during induction (Meurer *et al.*, 1996).

**Methods S1**

**Chlorophyll *a* fluorescence induction and light-induced PSI absorbance changes**

Chlorophyll *a* fluorescence induction kinetics and PSI absorbance changes at 820 nm were performed with leaves of WT, *mda1* mutants and complemented mutant plants using a Dual-PAM-100 System (Walz, Effeltrich, Germany) (Meurer *et al.*, 1996). $\Phi_{PSI}$, $\Phi_{PSI\ NA}$ and $\Phi_{PSI\ ND}$ were expressed as described (Klughammer & Schreiber, 1994). Measurements were taken from 2-week-old Arabidopsis plants grown on soil. Saturating light pulses were given in 20 s intervals during induction (Meurer et al., 1996). All parameters were taken from plants after 5 min induction using an actinic light intensity of 50 µmol photons $m^{-2}$ $s^{-1}$.

**Genome wide analyses of chloroplast transcriptome and translatome**

Chloroplast ribosome profiling analyses were performed as previously described (Trosch *et al.*, 2018). The data are provided in Table S3.

**Supporting Information references**


**Klughammer C, Schreiber U. 1994.** An improved method, using saturating light pulses, for the determination of photosystem I quantum yield via P700+-absorbance changes at 830 nm. *Planta* **192**(2): 261-268.

**Meurer J, Meierhoff K, Westhoff P. 1996.** Isolation of high-chlorophyll-fluorescence mutants of Arabidopsis thaliana and their characterisation by spectroscopy, immunoblotting and northern hybridisation. *Planta* **198**(3): 385-396.

**Ruwe H, Wang G, Gusewski S, Schmitz-Linneweber C. 2016.** Systematic analysis of plant mitochondrial and chloroplast small RNAs suggests organelle-specific mRNA stabilization mechanisms. *Nucleic Acids Res* **44**(15): 7406-7417.

**Trosch R, Barahimipour R, Gao Y, Badillo-Corona JA, Gotsmann VL, Zimmer D, Muhlhaus T, Zoschke R, Willmund F. 2018.** Commonalities and differences of chloroplast translation in a green alga and land plants. *Nat Plants* **4**(8): 564-575.

**Zhelyazkova P, Hammani K, Rojas M, Voelker R, Vargas-Suarez M, Borner T, Barkan A. 2012.** Protein-mediated protection as the predominant mechanism for defining processed mRNA termini in land plant chloroplasts. *Nucleic Acids Res* **40**(7): 3092-3105.